# Analytic Solutions of Two Electrons in Harmonic Confinement in an Optical Cavity


Chenhang Huang

Department of Physics and Astronomy

Vanderbilt University

*Supervisor*

Kálmán Varga

In partial fulfillment of the requirements for the honor degree of

*Bachelor of Arts in Physics*

December, 2021

# Acknowledgements

I would like to thank Professor Kálmán Varga for his consistent support and mentorship throughout my undergraduate career, without whom I cannot achieve the same rewarding research experience. I am grateful for the participation of my honor examination committee members, including Professor Scherrer, Professor Umar, and Professor Taylor. I would also express my gratitude to Professor Johns for his coordination of the examination.

# Abstract

The possibility to control quantum systems with photons has stimulated recent interest in the study of quantum optical systems. While simple classical quantum systems admit well-known solutions, analysis of light-coupling quantum regimes remains lacking. In this work, we obtain analytic solutions for a light-coupling electron pair in harmonic confinement in a cavity by separating center-of-mass (CM) and relative motions. The CM part can be calculated in closed form or by exact diagonalization of the Hamiltonian, and the relative part is quasi-exactly solvable. We analyze the 2D results produced by the exact diagonalization method and reach conclusions on the effects of different system parameters. We also present 1D numerical simulations by Stochastic Variational Method (SVM) using Explicitly Correlated Gaussian (ECG) bases, which agree with our analysis in 2D. Our analytic solutions may provide a valuable calibration point for simulations in the quantum optical regime.

# Contents

# 1. Introduction

The possibility to control quantum systems with photons has stimulated intense recent interest in the study of quantum optical systems [1]. The fundamental description of charged particles interacting with electromagnetic (EM) fields is based on quantum electrodynamics. This description is especially important when the light and matter are strongly coupled, such as in an optical cavity. Strong coupling between light and matter can occur when the interaction strength between a confined electromagnetic field and a molecular resonance exceeds the dissipation to the environment, leading to the formation of hybrid light-matter states known as polaritons. A typical optical cavity consists of two mirrors to trap light at certain frequencies as standing waves. The wavelength of light can be controlled by the length of the cavity (see Fig.1.1 for a 2D configuration) [2]. The light-matter coupling in these systems cannot be treated on the perturbative ground since the photons superimpose the electronic excitations. As a result, achieving exact solutions of the systems becomes difficult, leading to a lack of analytic calculations.

Several theoretical approaches have been proposed to tame the light-matter coupling problems. For example, by representing the wave function on the real space and the Fock space, the system of one electron coupled to a single photon mode in 2D can be solved by exact diagonalization of the Hamiltonian [3]. The same technique can be applied to the He, $HD^+$, and $H_2^+$ three-particle system, where exact diagonalization of the Hamiltonian permits a study on the Jaynes-Cummings limit for electronic and rovibrational transitions [4]. Reviews of the recent theoretical and experimental developments can be found in Refs. [5–7].

Although obtaining exact closed-form solutions prove to be difficult, quasi-

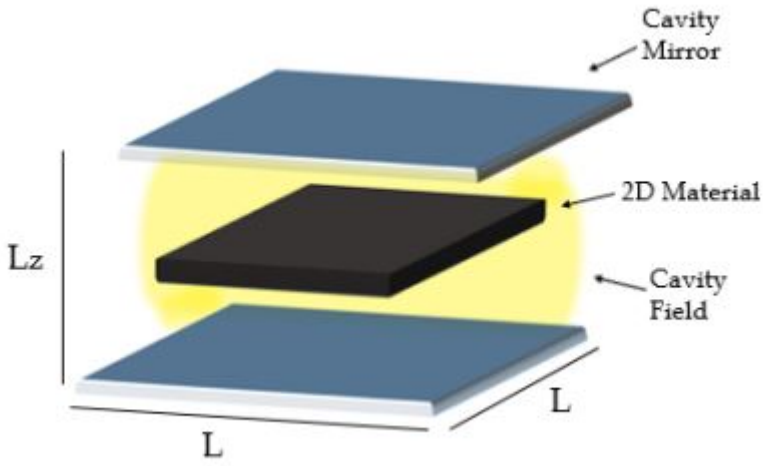


**Figure 1.1** Schematic depiction of a 2D material inside a cavity with mirrors of length $L$ and area $L^2$. The area of the material is also $L^2$.

exact solutions (QES) remain accessible. A QES is not a complete analytic account of the system but an analytic description for an (infinitely) countable set of system parameters. Indeed, quasi-exact solvability is the best alternative to exact solvability. Examples of QES systems include 2D harmoniums [8, 9], 2D spheriums [10, 11], electron pairs confined on 1D rings [12, 13], and hydrogen-like atoms in homogeneous magnetic fields [14].

In this work, we contribute to the collection of light-coupling QES systems. In particular, we consider a 2D electron pair coupled to a single photon mode in harmonic confinement and obtain the exact energy spectrum and corresponding wave functions. This system can be described by the Pauli-Fierz (PF) non-relativistic quantum electrodynamic (QED) Hamiltonian [15–20]. We will show that the Hamiltonian can be separated into the CM part and the relative part, and only the CM part couples to photons. The photon-electron interaction can be further decoupled and solved analytically. This 2D solution can be easily generalized to 3D with arbitrary photon modes.

Finally, we will present numerical simulation results in 1D from SVM and ECG bases. The characteristics of the two-electron wave functions can be clearly explained by the form of the analytic solutions. The same explanations can be generalized to many-particle systems as they possess similar properties to the two-electron case.

# 2. Formalism

## 2.1 Description of the system

The theoretical construction of SVM and ECG bases can be found in literature dealing with numerical techniques, such as Ref.[21]. In the following, we shall focus on the analytic solutions of two-electron systems. The Hartree atomic units ($\hbar = e = m_e = 1$) will be used throughout.

The simplest but complete picture of the optical cavity can be described by the PF QED Hamiltonian in the long-wavelength limit, where the cavity is much larger than the size of the system, such that the light has no spatial dependency. This PF Hamiltonian has been transformed into the length gauge. The derivation of the transformation is outlined in Appendix A, and a complete description can be found in Ref.[22]. Consider two particles with charges $z_1, z_2$ and positions $\mathbf{r_1}, \mathbf{r_2}$. The Humiliation dictating our light-coupling systems can be written as

$$H = H_e + H_{ph} = H_e + H_p + H_{ep} + H_d \tag{2.1}$$

where $H_e$ is the matter Hamiltonian, $H_{ph}$ describes the matter-light interactions. In particular, $H_{ph}$ is the sum of three terms: the photon Hamiltonian $H_p$, the matter-photon coupling Hamiltonian $H_{ep}$, and the matter-photon dipole self-interaction Hamiltonian $H_d$.

Explicitly, the Hamiltonians read

$$H_e = -\frac{1}{2}\nabla_1^2 + \frac{1}{2}\omega_0^2\mathbf{r}_1^2 - \frac{1}{2}\nabla_2^2 + \frac{1}{2}\omega_0^2\mathbf{r}_2^2 + \frac{z_1 z_2}{|\mathbf{r}_1 - \mathbf{r}_2|}, \tag{2.2}$$

$$H_{ph} = \frac{1}{2}\sum_{\alpha=1}^{N_p}\left[p_\alpha^2 + \omega_\alpha^2\left(q_\alpha - \frac{\boldsymbol{\lambda_\alpha}}{\omega_\alpha}\cdot\mathbf{D}\right)^2\right], \tag{2.3}$$

where the $p_\alpha = -i\sqrt{\frac{\omega_\alpha}{2}}(\hat{a}_\alpha - \hat{a}_\alpha^+)$ is the conjugate momentum operator, $q_\alpha = \frac{1}{\sqrt{2\omega_\alpha}}(\hat{a}_\alpha^+ + \hat{a}_\alpha)$ is the displacement field operator, and $\mathbf{D} = \sum_{i=1}^{N} z_i\mathbf{r}_i$ is the dipole operator. Evidently, $(\hat{a}^+, \hat{a})$ are the ladder operators, and $(\omega_a, \boldsymbol{\lambda_a})$ are the frequency and the coupling strength of the $\alpha$-th photon mode respectively.

The photon Hamiltonian appears quantized and harmonic in the Fock space

$$H_p = \sum_{\alpha=1}^{N_p}\left(\frac{1}{2}p_\alpha^2 + \frac{\omega_\alpha^2}{2}q_\alpha^2\right) = \sum_{\alpha=1}^{N_p}\omega_\alpha\left(\hat{a}_\alpha^+\hat{a}_\alpha + \frac{1}{2}\right), \tag{2.4}$$

the matter-photon Hamiltonian describes the first-order interaction between particles and light

$$H_{ep} = -\sum_{\alpha=1}^{N_p}\omega_\alpha q_\alpha\boldsymbol{\lambda_\alpha}\cdot\mathbf{D} = -\sum_{\alpha=1}^{N_p}\sqrt{\frac{\omega_\alpha}{2}}(\hat{a}_\alpha + \hat{a}_\alpha^+)\boldsymbol{\lambda_\alpha}\cdot\mathbf{D}, \tag{2.5}$$

and the dipole self-interaction term represents the effects of the polarization of electrons back onto the photon field

$$H_d = \frac{1}{2}\sum_{\alpha=1}^{N_p}\left(\boldsymbol{\lambda_\alpha}\cdot\mathbf{D}\right)^2. \tag{2.6}$$

## 2.2 Separation of the CM coordinate and the relative coordinate

For simplicity, we assume a system of two electrons and a single photon mode with isotropic photon coupling; namely, $z_1 = z_2 = 1$, $N_p = 1$, and $\boldsymbol{\lambda_\alpha} = (\lambda, \lambda, 0)$. By introducing the CM coordinate and the relative coordinate

$$\begin{aligned}\mathbf{r} &= \mathbf{r}_2 - \mathbf{r}_1,\\ \mathbf{R} &= \tfrac{1}{2}\left(\mathbf{r}_1 + \mathbf{r}_2\right),\end{aligned} \tag{2.7}$$

we can rewrite two terms of the total Hamiltonian

$$\begin{aligned} H_e + H_d &= -\nabla_{\mathbf{r}}^2 + \frac{1}{4}\omega_0^2 \mathbf{r}^2 + \frac{z_1 z_2}{r} - \frac{1}{4}\nabla_{\mathbf{R}}^2 + \omega_0^2 \mathbf{R}^2 + 2\left(\boldsymbol{\lambda}\cdot\mathbf{R}\right)^2 \\ &\equiv H_{\mathbf{r}} + H_{\mathbf{R}}, \end{aligned} \tag{2.8}$$

and the corresponding eigenvalue problem is

$$\left(H_{\mathbf{r}} + H_{\mathbf{R}}\right)\Phi(\mathbf{r},\mathbf{R}) = (\epsilon+\eta)\Phi(\mathbf{r},\mathbf{R}) = (\epsilon+\eta)\varphi(\mathbf{r})\xi(\mathbf{R}). \tag{2.9}$$

The relative part $H_r$ and the CM part $H_R$ explicitly read

$$\frac{1}{2}H_{\mathbf{r}}\,\varphi(\mathbf{r}) = \left[-\frac{1}{2}\nabla_{\mathbf{r}}^2 + \frac{1}{2}\omega_{\mathbf{r}}^2\mathbf{r}^2 + \frac{1}{2}\frac{1}{r}\right]\varphi(\mathbf{r}) = \varepsilon'\varphi(\mathbf{r}), \tag{2.10}$$

where $\omega_{\mathrm{r}} = \frac{1}{2}\omega_0$ and $\varepsilon' = \frac{1}{2}\varepsilon$, and

$$2H_{\mathbf{R}}\,\xi(\mathbf{R}) = \left[-\frac{1}{2}\nabla_{\mathbf{R}}^2 + \frac{1}{2}\omega_{\mathbf{R}}^2\mathbf{R}^2 + 4(\boldsymbol{\lambda}\cdot\mathbf{R})^2\right]\xi(\mathbf{R}) = \eta'\,\xi(\mathbf{R}), \tag{2.11}$$

where $\omega_{\mathbf{R}} = 2\omega_0$ and $\eta' = 2\eta$.

In 2D, using $\mathbf{R} = (X, Y)$ one can rewrite $H_{\mathbf{R}}$ as (in 3D one simply has to multiply the CM wave function with a quantum harmonic oscillator function of frequency $2\omega_0$ in the $Z$-direction)

$$2H_{\mathbf{R}} = -\frac{1}{2}\frac{\partial^2}{\partial X^2} - \frac{1}{2}\frac{\partial^2}{\partial Y^2} + \frac{1}{2}\omega_X^2 X^2 + \frac{1}{2}\omega_Y^2 Y^2 + \frac{1}{2}\omega_{XY}^2 XY, \tag{2.12}$$

where

$$\omega_X^2 = \omega_Y^2 = \omega_{\mathbf{R}}^2 + 8\lambda^2, \qquad \omega_{XY}^2 = 16\lambda^2. \tag{2.13}$$

Using a unitary transformation

$$U = \frac{X+Y}{\sqrt{2}}, \qquad V = \frac{-X+Y}{\sqrt{2}}, \tag{2.14}$$

we decouple the CM part

$$\begin{aligned} 2H_{\mathbf{R}} &= -\frac{1}{2}\frac{\partial^2}{\partial U^2} - \frac{1}{2}\frac{\partial^2}{\partial V^2} + \frac{1}{2}\omega_U^2 U^2 + \frac{1}{2}\omega_V^2 V^2 \\ &\equiv H_U + H_V, \end{aligned} \tag{2.15}$$

where

$$\omega_U^2 = \frac{1}{2}(\omega_X^2 + \omega_{XY}^2 + \omega_Y^2) = \omega_R^2 + 16\lambda^2, \tag{2.16}$$

$$\omega_V^2 = \frac{1}{2}(\omega_X^2 - \omega_{XY}^2 + \omega_Y^2) = \omega_R^2. \tag{2.17}$$

Clearly, this Hamiltonian just represents a system of two non-interacting quantized harmonic oscillators, yielding the ground state energy

$$\eta = \frac{1}{2}\left(\omega_0 + \sqrt{\omega_0^2 + 4\lambda^2}\right). \tag{2.18}$$

More conveniently, we define

$$u = \sqrt{2}U,\ v = \sqrt{2}V,\ \omega_u = \frac{\omega_U}{2},\ \omega_v = \frac{\omega_V}{2} \tag{2.19}$$

so that $H_{\mathbf{R}} = H_u + H_v$. The wave function of the system is therefore the product of the $u$-harmonic wave function and the $v$-harmonic wave function

$$\xi(\mathbf{R}) = \phi_k(u)\phi_l(v), \tag{2.20}$$

where $\phi_k$ is the $k$-th eigenfunction of the one-dimensional quantized harmonic oscillator,

$$\begin{aligned} \phi_k(u) &= \left(\frac{\sqrt{\omega_u}}{\sqrt{\pi}\,2^k k!}\right)^{\frac{1}{2}} \mathrm{e}^{-\frac{\omega_u}{2}u^2} H_k(\sqrt{\omega_u}\,u), \\ \phi_k(v) &= \left(\frac{\sqrt{\omega_v}}{\sqrt{\pi}\,2^k k!}\right)^{\frac{1}{2}} \mathrm{e}^{-\frac{\omega_v}{2}v^2} H_k(\sqrt{\omega_v}\,v), \end{aligned} \tag{2.21}$$

where $H_k$ is the Hermite polynomial. It is also straightforward to generalize this decoupling transformation to $N_p$ photon modes (see Ref.[23]).

The relative part admits quasi-exact series solution for a countably infinite number of frequencies $\omega_0$. For example, if $\omega_0 = 1$, we compute $\epsilon = 2$. However, the calculations become more tedious. The details of the calculations and tables of available energy spectrum can be found in Appendix B.

## 2.3 Separation of the photon-electron coupling

Now, we bring in the remaining two terms of the Hamiltonian. For the current simplified two-electron systems, the matter-photon Hamiltonian (2.5) reduces to

$$H_{ep} = -\sqrt{\frac{\omega}{2}}(\hat{a} + \hat{a}^{+})\lambda D, \qquad D = 2\sqrt{2}u, \tag{2.22}$$

and the total Hamiltonian (2.1) writes

$$H = H_u + \omega\left(\hat{a}^{+}\hat{a} + \frac{1}{2}\right) - 2\omega\sqrt{2}\lambda uq. \tag{2.23}$$

There are two possible approaches to analytically solve this total Hamiltonian (2.23). First, we will use another unitary transformation to eliminate the coupling term and again find the resulting Hamiltonian to be the representation of two non-interacting quantized harmonic oscillators. Second, we can express this Hamiltonian in the product space of the real spatial $u$-space with the Fock space $|n\rangle$. The first approach produces closed-form solutions, while the second one generates answers in a more convenient space.

### 2.3.1 Separation by a unitary transformation

Define the rotation

$$\begin{aligned} s &= u \sin\alpha + q \cos\alpha, \\ t &= -u \cos\alpha + q \sin\alpha, \end{aligned} \tag{2.24}$$

the coupling term in (2.23) can be eliminated by choosing

$$\tan 2\alpha = \frac{4\omega\lambda}{\chi}, \tag{2.25}$$

where $\chi = \omega_u^2 - \omega^2$, and $\omega_u^2 = \omega_0^2 + 4\lambda^2$ (this construction resembles the one in Sec.2.2, but for more details, see Ref.[24]).

As promised, the decoupled Hamiltonian again describes two non-interacting quantized harmonic oscillators

$$H = -\frac{1}{2}\frac{\partial^2}{\partial s^2} + \frac{1}{2}\omega_s s^2 - \frac{1}{2}\frac{\partial^2}{\partial t^2} + \frac{1}{2}\omega_t t^2, \tag{2.26}$$

where

$$\begin{aligned} \omega_s &= |\sin\,\alpha|\,\sqrt{\omega_0^2 + (2\lambda - \omega/\tan\,\alpha)^2}, \\ \omega_t &= |\cos\,\alpha|\,\sqrt{\omega_0^2 + (2\lambda + \omega\tan\,\alpha)^2}, \end{aligned} \tag{2.27}$$

so the energy spectrum of the entire system is explicitly

$$E(n_s, n_t) = (n_s + \frac{1}{2})\omega_s + (n_t + \frac{1}{2})\omega_t \tag{2.28}$$

with the corresponding wave function

$$\phi_{n_s n_t}(s,t) = \phi_{n_s}(s)\phi_{n_t}(t). \tag{2.29}$$

Notice that the transformed coordinates $(s,t)$ (shifted Fock states) now mix the spatial part with the Fock states, an inconvenient form for direct analysis.

Incidentally, the well-known effect of Rabi splitting in the Jaynes-Cummings model can be observed through this simple calculation. Namely, $\omega_s$ and $\omega_t$ switch roles at resonant frequency $\chi \to 0$, and the transition energy at this frequency can be computed for experimental comparison. For a more detailed discussion on this subject, see Ref.[23].

### 2.3.2 Separation by exact diagonalization

Working with the basis $\phi_k(u) \otimes |n\rangle$, we can evaluate the $u$-part in the real space and the $q$-part in the Fock space,

$$\langle\phi_i|u|\phi_j\rangle = \frac{1}{\sqrt{2\omega_u}} D_{ij}. \tag{2.30}$$

$$\langle\phi_i|H_u|\phi_j\rangle = (j + \frac{1}{2})\omega_u\delta_{ij}, \tag{2.31}$$

$$\langle n|\,\omega\left(\hat{a}^+\hat{a} + \frac{1}{2}\right)|m\rangle = (n + \frac{1}{2})\omega\delta_{nm}, \tag{2.32}$$

$$\langle m|q|n\rangle = \frac{1}{\sqrt{2\omega}} D_{mn}, \tag{2.33}$$

where we have defined the auxiliary matrix $D_{mn}$ as

$$D_{mn} = \begin{pmatrix} 0 & \sqrt{1} & 0 & 0 & 0 & \dots \\ \sqrt{1} & 0 & \sqrt{2} & 0 & 0 & \dots \\ 0 & \sqrt{2} & 0 & \sqrt{3} & 0 & \dots \\ 0 & 0 & \sqrt{3} & 0 & \sqrt{4} & \dots \\ 0 & 0 & 0 & \sqrt{4} & 0 & \dots \\ \vdots & \vdots & \vdots & \vdots & \vdots & \ddots \end{pmatrix}. \tag{2.34}$$

Therefore, the matrix element of the Hamiltonian in this basis is given by

$$\langle m, \phi_i | H | n, \phi_j \rangle = \delta_{mn}\delta_{ij}(j + \frac{1}{2})\omega_u + \delta_{mn}\delta_{ij}(n + \frac{1}{2})\omega + \sqrt{\frac{2\omega}{\omega_U}}\,\lambda\, D_{mn}D_{ij}. \tag{2.35}$$

Evidently, this Hamiltonian matrix appears extremely sparse. As a result, numerical diagonalization at even a large cut-off of the matrix dimension remains efficient. The eigen-energies can be exactly calculated, and the corresponding wave functions have the form

$$\xi_k(\mathbf{R}) = \sum_{n=0}^{K_n} \left( \sum_{j=0}^{K_u} c_{j,n}^k \psi_n(\mathbf{R}) \right) |n\rangle = \sum_{j=0}^{K_u} \left( \sum_{n=0}^{K_n} c_{j,n}^k |n\rangle \right) \psi_j(\mathbf{R}), \tag{2.36}$$

where

$$\psi_j(\mathbf{R}) = \phi_i(v)\phi_j(u) \tag{2.37}$$

is the spatial wave function given in Sec.2.2, $c_{j,n}^k$ is some linear combination coefficient associated with the basis, and $K_u, K_n$ are reasonable cut-offs of the matrix dimension. In practice, a modest choice of $K_u, K_n$ yields well-converged energies and wave functions.

# 3. Results & Discussion

## 3.1 2D and 3D electron pairs

The unitary transformation in Sec.2.3.1 and the exact diagonalization in Sec.2.3.2 give identical results if the matrix dimension of (2.35) is sufficiently large. In this section, we only present the energy spectrum and the wave functions obtained from the exact diagonalization method, since this method produces densities already in the basis of the real space and the photon space. Specifically, we proceed by selecting an oscillator frequency $\omega_0$ from the table of Appendix B, calculating the corresponding relative wave function as described in Appendix B, and multiplying this relative wave function with the CM component (2.36). We assume the lowest state $i = 0$ in the $v$-direction in (2.37). With this configuration, the excitation of the system is determined by the CM excitation $j$ and the photon excitation.

We only present outcomes in 2D since it is easier to visualize the densities on a plane. Moreover, it suffices to analyze the principle characteristics of the 2D results, since one can trivially incorporate the quantized harmonic oscillator in the $Z$-direction (Sec.2.2) to transform to 3D.

### 3.1.1 Spin-singlet states

First, we show the spin-singlet case using $\omega_0 = 1$. The energy of the relative motion is $\epsilon = 2$ in this case (see the Table in Appendix B). Fig.3.1 shows the wave functions of different spin-singlet states. The state with $j = 0$ CM wave function is spherically symmetric for small $\lambda$ ($\lambda = 0.5$, Fig.3.1a) but appears squashed

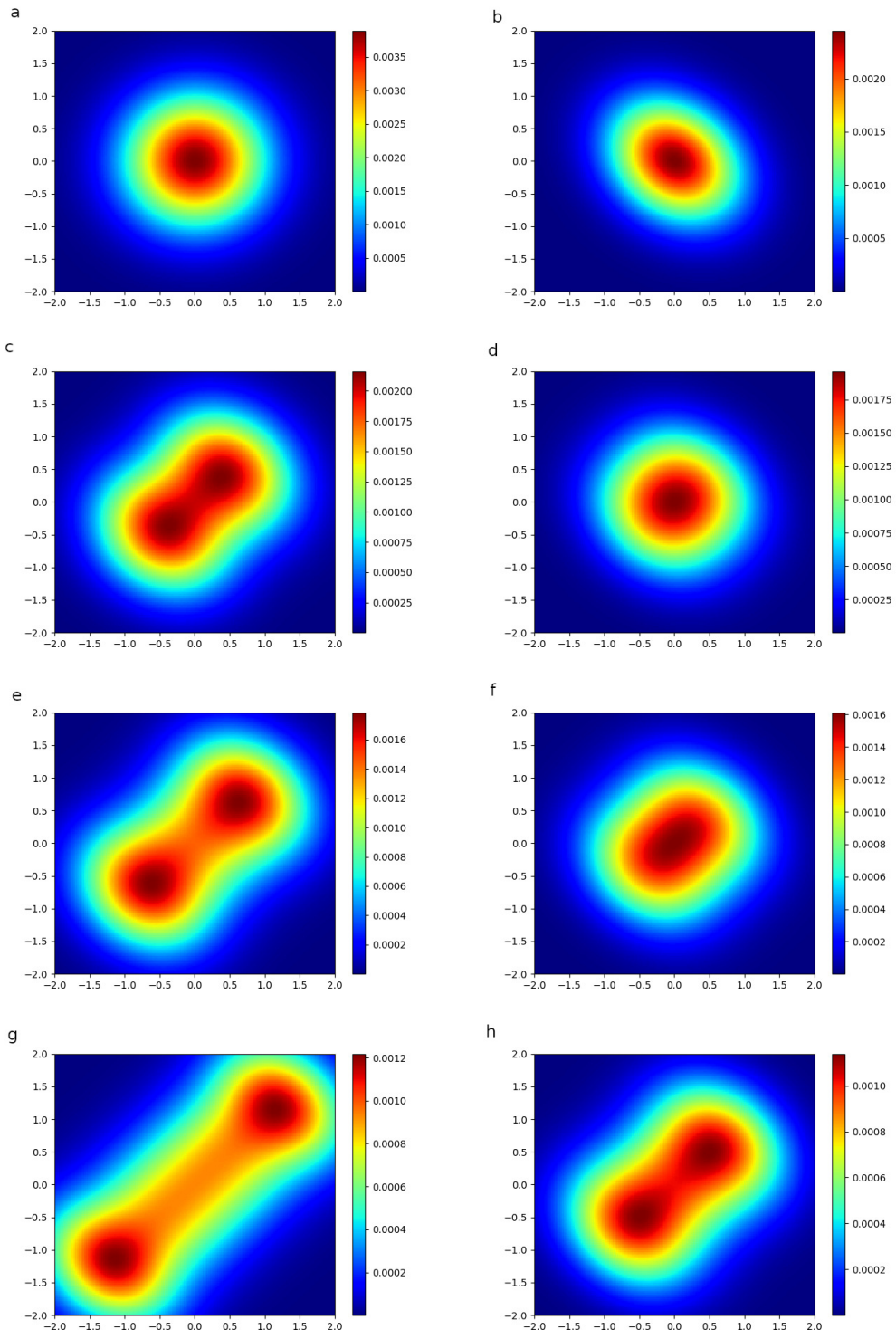


**Figure 3.1** Two-dimensional densities of two electrons confined in a harmonic potential with $\omega_0 = 1$ a.u., $\omega = 0.5$ a.u., and spin $S = 0$ for different $j$ (CM quantum number) and $\lambda$ values. First row: j=0, (a) $\lambda = 0.5$, (b) $\lambda = 2$. Second row: j=1, (c) $\lambda = 0.5$, (d) $\lambda = 2$. Third row: j=2, (e) $\lambda = 0.5$, (f) $\lambda = 2$. Fourth row: j=5, (g) $\lambda = 0.5$, (h) $\lambda = 2$. The $x$ axis is horizontal, and the $y$ axis is vertical. The color bar shows the probability density.

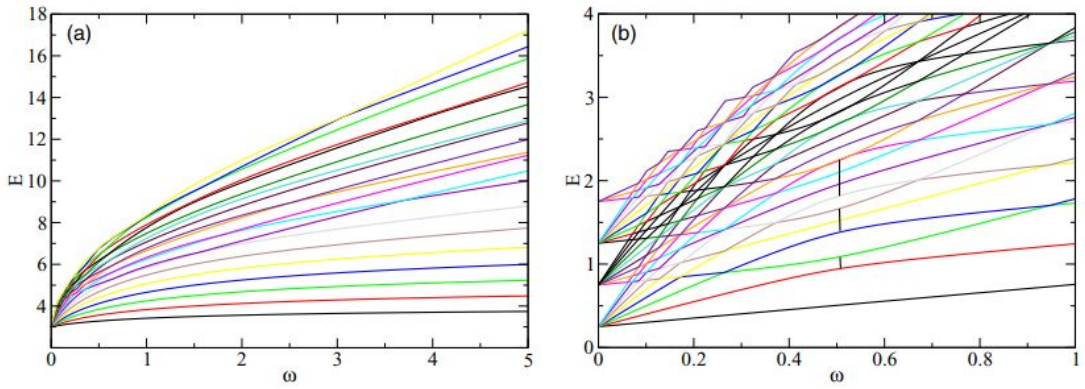


**Figure 3.2** The energy levels as a function of $\omega$ for different $\lambda$ values (the confinement strength is $\omega_0 = 0.5$ a.u.): (a) $\lambda = \sqrt{\omega}$ and (b) $\lambda = \sqrt{\omega}/10$. The energy of the relative motion is added to the energy in (a) but not in (b)

along the diagonal for larger $\lambda$ ($\lambda = 2$, Fig.3.1b), as the anharmonicity dominates ($\omega_v << \omega_u$). This diagonal direction is set by the choice of $\boldsymbol{\lambda} = (\lambda, \lambda)$, and other choices of $\boldsymbol{\lambda}$ will change the direction (see Ref.[23]).

For $j = 1$, the CM state is multiplied by $u$ ($H_1(\sqrt{\omega_u}\, u) = 2\sqrt{\omega_u}\, u$) and becomes elongated diagonally due to the first-order Hermite polynomial (Fig.3.1c). As $\lambda$ increases, again the anharmonicity dominates, which neutralizes the elongation (Fig.3.1d).

The same process continues for higher $j$ values. The diagonal elongation increases due to the higher $H_j(\sqrt{\omega_u}u)$ polynomials (Figs.3.1e and 3.1g), but stronger anharmonicity of $\omega_u$ from higher $\lambda$ values counteracts the elongation (Figs.3.1f and 3.1h). Solutions with other $\omega_0$ values show very similar behaviors.

Figure.3.2 shows the lowest 30 states in the singlet state energy spectrum as a function of photon frequency $\omega$, where we use a coupling strength $\lambda = x\sqrt{\omega}$. Different lines correspond to different excited states, some due to photon excitation while the others due to CM excitations. For $x = 1$ (Fig.3.2a), some states (primarily photon states) move linearly up with $\omega$ for small frequencies, while other states (primarily CM states) only slowly increase with $\omega$. Incidentally, in the absence of the photon-electron coupling (which is not the case in Fig.3.2), both the photon states and the CM states need to display linear correlation with $\omega$ in general. For $x = 1/10$ (Fig.3.2b), the vertical lines represent the Rabi splitting introduced in Sec.2.3.1. The vertical lines only appear in Fig.3.2b but not in Fig.3.2a, since calculations in Sec.2.3.1 can prove that Rabi splittings only occur at small $\lambda$ (see

Ref.[23]).

### 3.1.2 Spin-triplet states

In the spin-triplet case in 2D we choose $\omega_0 = 1/3$, and the energy of the relative motion is $\epsilon = 1$ in this case. Fig.3.3 shows the wave functions for different spin-triplet states. Noticeably, one fundamental distinction between the triplet states and the singlet states is the two-peak structure in Fig.3.3b, where $j = 0$ and $\lambda = 0.5$, in contrast to the monotone structure in Fig.3.1a. Moreover, this two-peak characteristic persists for stronger anharmonicity ($\lambda = 1$, Fig.3.3c) due to the Pauli exclusion principle.

The effects of varying $j$ and $\lambda$ resemble those in the singlet state: higher $j$ values extend the system along the diagonal because of the higher-order Hermite polynomials, while increased $\lambda$ confines the system more compactly. A three-peak and even a four-peak structure appear in Fig.3.3d, g, and j due to the diagonal elongation, but these structures can be suppressed with stronger $\omega_u$ confinement. In general, the same structure for a pair of values $(j, \lambda)$ will appear later for another pair of larger values.

Indeed, it is also possible to generalize our analysis to individual photon space or individual CM space by fixing the photon number $n$ or CM number $j$ in (2.36) respectively. Fig.3.4 shows example plots of the density functions in different photon spaces.

## 3.2 1D electron pairs

In the remaining, we present simulations of 1D few-electron systems harmonically confined in an optical cavity generated with SVM and ECG bases. We will show that our analysis of the structure of the 2D systems also applies in 1D.

The same formalism in Chap.2 can be reused in 1D. Therefore, we feed the simulation with the same Hamiltonian (2.1), with the Coulomb term being replaced by the soft Coulomb

$$V(x_i - x_j) = \frac{1}{\sqrt{(x_i - x_j)^2 + 1}}. \tag{3.1}$$

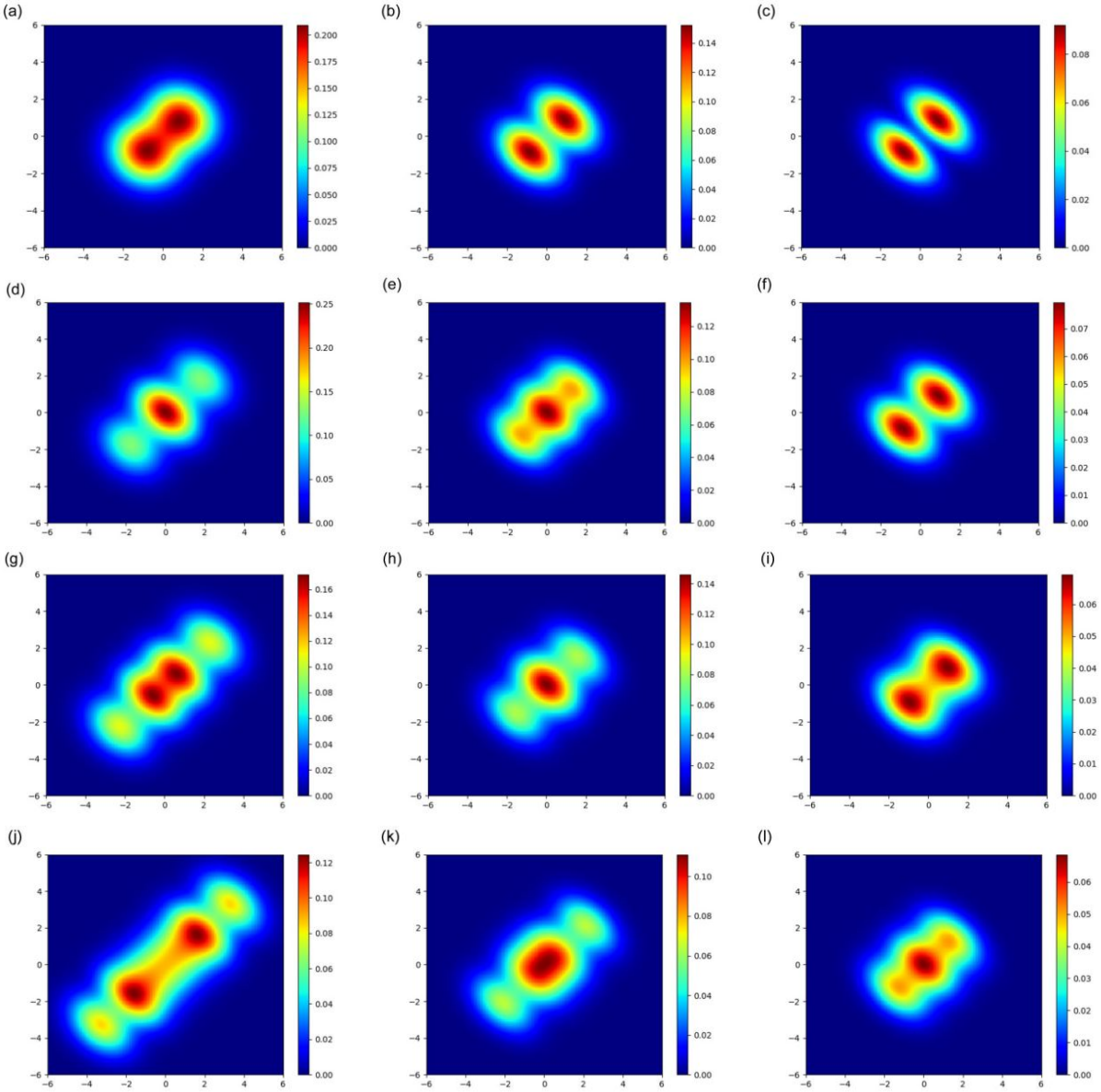


**Figure 3.3** Two-dimensional densities of two electrons confined by a harmonic potential with $\omega_0 = 1/3$, $\omega = 0.5$ a.u. and spin $S = 1$ for different $j$ (CM quantum number) and $\lambda$ values. First row: $j = 0$, (a) $\lambda = 0.01$, (b) $\lambda = 0.5$, (c) $\lambda = 2$. Second row: $j = 1$, (d) $\lambda = 0.01$, (e) $\lambda = 0.5$, (f) $\lambda = 2$. Third row: $j = 2$, (g) $\lambda = 0.01$, (h) $\lambda = 0.5$, (i) $\lambda = 2$. Fourth row: $j = 5$, (j) $\lambda = 0.01$, (k) $\lambda = 0.5$, (l) $\lambda = 2$. The $x$ axis is horizontal, and the $y$ axis is vertical. The color bar shows the probability density.

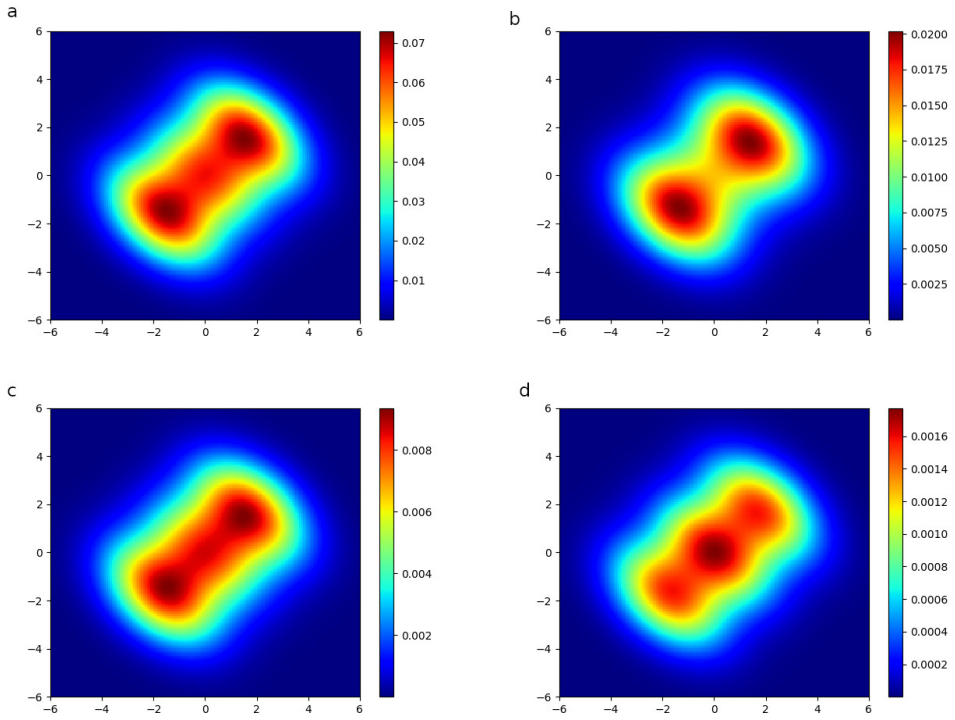


**Figure 3.4** Two-dimensional density $\Phi(\mathbf{r}, \mathbf{R})^2$ for the $S = 1$ case, (a) total density, (b) density in the $n = 1$ space, (c) density in the $n = 3$ space, (d) density in the $n = 5$ space. ($\omega_0 = 0.18055$ a.u., $\omega = 1$ a.u. and $\lambda = 1$ a.u.).

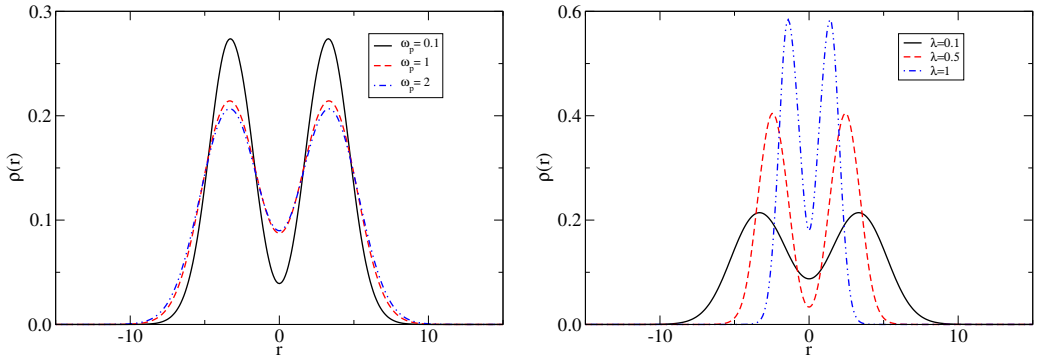


**Figure 3.5** Electron density of the two-electron $S = 1$ system coupled to light. Left $\lambda = 0.1$ a.u., right $\omega_p = 1$ a.u.

This replacement is a necessary common practice among simulations of 1D systems, due to the singular nature of the Coulomb potential when particles approach each other [25].

Fig.3.5 shows the relative wave functions of an electron pair in the triplet $S = 1$ state, where we have denoted the harmonic confinement strength as $\omega = 0.1$, the photon frequency as $\omega_p$, and the electron-photon coupling strength as $\lambda$. The CM component has been discarded since it lacks the interesting structures observed in 2D (see (2.11)). As a result, the excitation of the CM part does not affect the densities. Nevertheless, effects of $\lambda$ resemble those in 2D: stronger $\lambda$ restricts the system more compactly (Fig.3.5b). The structure of the system has diminishing dependence on $\omega_p$, since the Hamiltonian (2.23) is linearly correlated with $\omega_p$ but quadratically associated with $\lambda$.

Indeed, there is no limit to the size of the system. As we are not pursuing analytic solutions, larger systems can also be efficiently calculated with SVM. For example, Fig.3.6 and 3.7 demonstrate the wave functions of a three-electron system and a four-electron system respectively. It is clear that many trends unveiled in 2D remain true in 1D. On the one hand, for spin-polarized cases ($S = 1.5$ for three electrons and $S = 2$ for four electrons), the number of density peaks match the number of electrons at strong confinement $\lambda$ due to the Pauli exclusion principle (Fig.3.6d and 3.7d). On the other hand, for non-spin-polarized scenarios, one or more peaks may be suppressed by the electron-photon coupling (Fig.3.6b and 3.7b). The energy spectrum of these systems can be found in Appendix C.

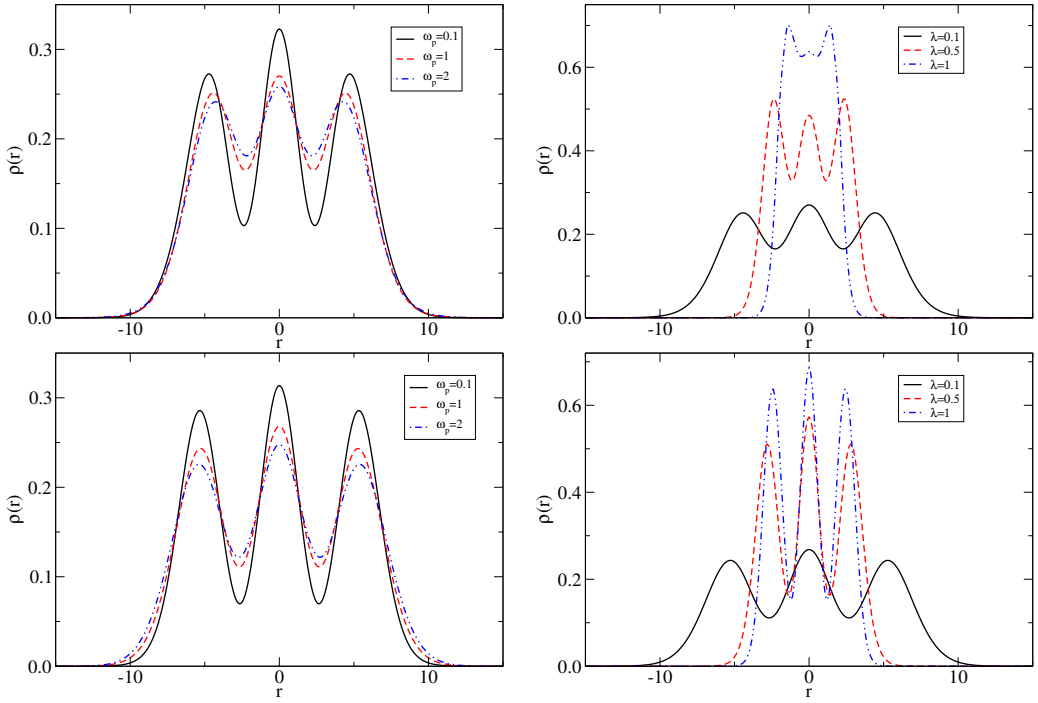


**Figure 3.6** Electron density of the three-electron system coupled to light. Top $S = 1/2$, bottom $S = 3/2$; left $\lambda = 0.1$ a.u., right $\omega_p = 1$ a.u.

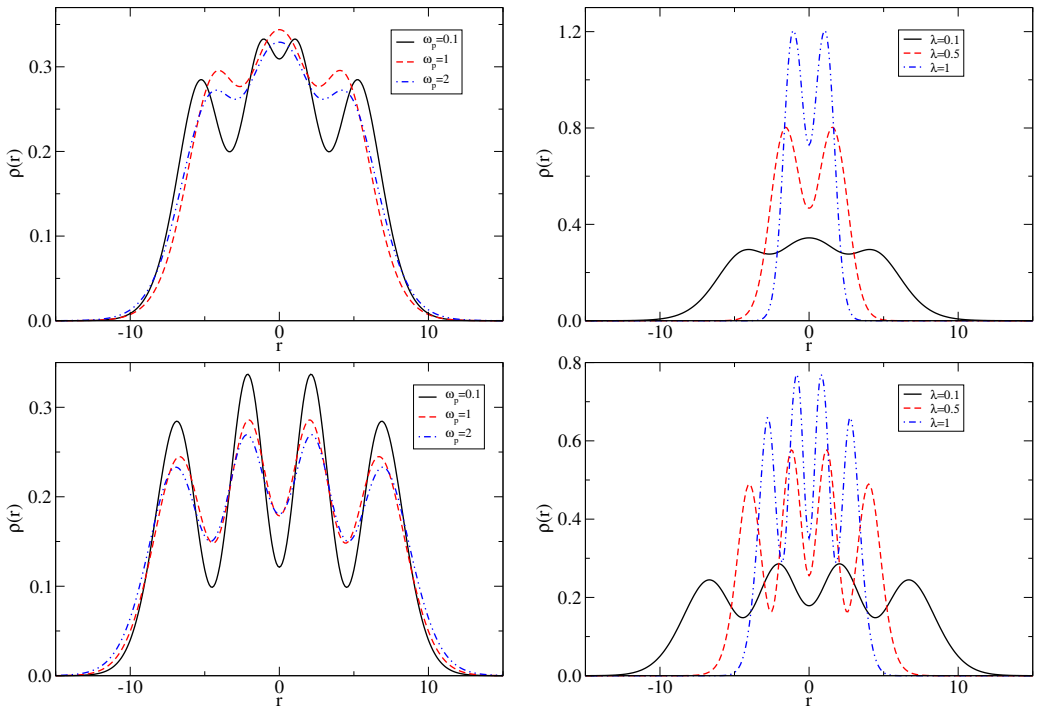


**Figure 3.7** Electron density of the four-electron system coupled to light. Top $S = 0$, bottom $S = 2$; left $\lambda = 0.1$ a.u., right $\omega_p = 1$ a.u.

# 4. Conclusions

For a two-electron system harmonically confined in an optical cavity, the wave function can be separated into the CM and relative coordinates. The light coupling only interacts with the CM coordinates. We have demonstrated that the CM part can be analytically solved by a unitary transformation into the shifted Fock states or by exact diagonalization of the total Hamiltonian, and the relative part admits quasi-exact series solutions. The method of exact diagonalization permits direct analysis of the wave functions, where we conclude that their structures primarily depend on the strength of the competing forces of light coupling and CM excitation. The same analysis applies in 1D and our conclusions agree with the results generated by SVM simulations.

This work provides an analytic solution to the difficult quantum optical system and might serve as a valuable calibration for numerical methods in this regime. These analytic solutions can be generalized to larger systems with $N$ electrons, but the relative part needs to be solved numerically.

# A. Length Gauge Transformation of the PF Hamiltonian

The usual PF Hamiltonian describing electron-photon coupling is

$$\begin{aligned}\hat{H} &= \frac{1}{2m}\sum_{j=1}^{N}\left(i\hbar\nabla_j + \frac{e}{c}\hat{\mathbf{A}}(\mathbf{r}_j)\right)^2 + \frac{1}{4\pi\epsilon_0}\sum_{j<k}^{N}\frac{e^2}{|\mathbf{r}_j-\mathbf{r}_k|} + \sum_{j=1}^{N} v_{ext}(\mathbf{r}_j) \\ &+ \sum_{\mathbf{n},\lambda}\left[-\frac{\hbar\omega_n}{2}\frac{\partial^2}{\partial q_{\mathbf{n},\lambda}^2} + \frac{\hbar\omega_n}{2}q_{\mathbf{n},\lambda}^2\right], \end{aligned} \tag{A.1}$$

where we neglected the Pauli term, i.e., $\hat{\boldsymbol{\sigma}}\cdot\hat{\mathbf{B}}(\mathbf{r})$, where $\hat{\boldsymbol{\sigma}}$ is a vector of the standard Pauli matrices and $\hat{\mathbf{B}}(\mathbf{r})$ corresponds to the magnetic field, since it will not contribute in the long-wavelength limit. The third term corresponds to an external scalar potential that acts on the electrons, such as the attractive potential of the nuclei.

The quantized vector potential of the electromagnetic wave in the Coulomb gauge (velocity gauge) reads

$$\hat{\mathbf{A}}(\mathbf{r}) = \left(\frac{\hbar c^2}{\epsilon_0 L^3}\right)^{\frac{1}{2}}\sum_{\mathbf{n},\lambda}\frac{\boldsymbol{\epsilon}_{\mathbf{n},\lambda}}{\sqrt{2\omega_n}}\left[\hat{a}_{\mathbf{n},\lambda}e^{i\mathbf{k}_n\cdot\mathbf{r}} + \hat{a}_{\mathbf{n},\lambda}^{\dagger}e^{-i\mathbf{k}_n\cdot\mathbf{r}}\right], \tag{A.2}$$

where $\omega_n = c|\mathbf{n}|(2\pi/L)$ are the allowed frequencies in a cavity box of length $L$, $\epsilon_0$ the vacuum permittivity, $\lambda$ the two transversal polarization directions and $\boldsymbol{\epsilon}_{\mathbf{n},\lambda}$ are the transversal polarization vectors of each photon mode which are perpendicular to the direction of propagation $\mathbf{k}_n$.

In the long-wavelength limit, we can neglect the spatial variation of the electromagnetic field $e^{\pm i\mathbf{k}_n\cdot\mathbf{r}} \approx 1$. The vector potential $\hat{\mathbf{A}}(\mathbf{r})$ in this limit is given by

$$\hat{\mathbf{A}} = \sum_{\alpha=1}^{M} \frac{C\boldsymbol{\epsilon}_\alpha}{\sqrt{\omega_\alpha}} q_\alpha \qquad \text{where} \qquad C = \left(\frac{\hbar c^2}{\epsilon_0 L^3}\right)^{\frac{1}{2}}. \tag{A.3}$$

As a result, (A.1) becomes

$$\begin{aligned} \hat{H}_V &= \frac{1}{2m}\sum_{j=1}^{N}\left[-\hbar^2\nabla_j^2 + 2i\frac{e\hbar}{c}\hat{\mathbf{A}}\cdot\nabla_j + \frac{e^2}{c^2}\hat{\mathbf{A}}^2\right] + \frac{1}{4\pi\epsilon_0}\sum_{j<k}^{N}\frac{e^2}{|\mathbf{r}_j - \mathbf{r}_k|} \\ &+ \sum_{j=1}^{N} v_{ext}(\mathbf{r}_j) + \sum_{\alpha=1}^{M}\left[-\frac{\hbar\omega_\alpha}{2}\frac{\partial^2}{\partial q_\alpha^2} + \frac{\hbar\omega_\alpha}{2}q_\alpha^2\right]. \end{aligned} \tag{A.4}$$

Transform this Hamiltonian into the length gauge by the unitary transformation

$$\hat{H}'_L = \hat{U}^\dagger \hat{H}_V \hat{U}, \qquad \hat{U} = \exp\left[\frac{i}{\hbar}\frac{e}{c}\hat{\mathbf{A}}\cdot\mathbf{R}\right], \tag{A.5}$$

where $\mathbf{R} = \sum_{i=1}^{N}\mathbf{r}_i$. We reach the form

$$\begin{aligned} \hat{H}'_L = &-\frac{\hbar^2}{2m}\sum_{i=1}^{N}\nabla_i^2 + \frac{1}{4\pi\epsilon_0}\sum_{i<j}^{N}\frac{e^2}{|\mathbf{r}_i - \mathbf{r}_j|} + \sum_{i=1}^{N} v_{ext}(\mathbf{r}_i) \\ &+ \sum_{\alpha=1}^{M}\left[-\frac{\hbar\omega_\alpha}{2}\frac{\partial^2}{\partial q_\alpha^2} + \frac{\hbar\omega_\alpha}{2}q_\alpha^2 - i\frac{\sqrt{\omega_\alpha}eC\boldsymbol{\epsilon}_\alpha\cdot\mathbf{R}}{c}\frac{\partial}{\partial q_\alpha} + \frac{\hbar\omega_\alpha}{2}\left(\frac{eC\boldsymbol{\epsilon}_\alpha\cdot\mathbf{R}}{\hbar c\sqrt{\omega}_\alpha}\right)^2\right]. \end{aligned} \tag{A.6}$$

Finally, by swapping the conjugate momentum with the photon coordinate $i\frac{\partial}{\partial q_\alpha} \to p_\alpha$ and $q_\alpha \to -i\frac{\partial}{\partial p_\alpha}$, we reach the final Hamiltonian in the length gauge

$$\begin{aligned} \hat{H}_L &= -\frac{\hbar^2}{2m}\sum_{i=1}^{N}\nabla_i^2 + \frac{1}{4\pi\epsilon_0}\sum_{i<j}^{N}\frac{e^2}{|\mathbf{r}_i - \mathbf{r}_j|} + \sum_{i=1}^{N} v_{ext}(\mathbf{r}_i) \\ &+ \sum_{\alpha=1}^{M}\left[-\frac{\hbar\omega_\alpha}{2}\frac{\partial^2}{\partial p_\alpha^2} + \frac{\hbar\omega_\alpha}{2}\left(p_\alpha - \frac{Ce}{\hbar c}\frac{\boldsymbol{\epsilon}_\alpha\cdot\mathbf{R}}{\sqrt{\omega_\alpha}}\right)^2\right], \end{aligned} \tag{A.7}$$

where it explicitly contains the electron-photon interaction

$$\hat{V}_{int} = -\sum_{\alpha=1}^{M}\left(\boldsymbol{\lambda}_\alpha\cdot\mathbf{R}\right)p_\alpha \qquad \text{where} \qquad \boldsymbol{\lambda}_\alpha = \frac{\sqrt{\omega}_\alpha eC\boldsymbol{\epsilon}_\alpha}{c}, \tag{A.8}$$

and the dipole self-energy

$$\hat{\varepsilon}_{dip} = \sum_{\alpha=1}^{M}\frac{\hbar\omega_\alpha}{2}\left(\frac{eC}{c\hbar}\frac{\boldsymbol{\epsilon}_\alpha\cdot\mathbf{R}}{\sqrt{\omega_\alpha}}\right)^2. \tag{A.9}$$

# B. Solutions of Relative Motion

## B.1 2D systems

The relative Hamiltonian is

$$\left[-\frac{1}{2}\nabla_{\mathbf{r}}^2+\frac{1}{2}\omega_{\mathbf{r}}^2\mathbf{r}^2+\frac{1}{2}\frac{1}{r}\right]\varphi(\mathbf{r})=\varepsilon'\varphi(\mathbf{r}). \tag{B.1}$$

In polar coordinates $\mathbf{r}=(r,\alpha)$, we assume the following ansatz and make the change of variables

$$\begin{aligned}\varphi(\mathbf{r})&=\frac{e^{im\alpha}}{\sqrt{2\pi}}\frac{u(r)}{r^{1/2}}\text{ , where } m\in\mathbb{Z},\\ \varepsilon''&=2\varepsilon'/\omega_r,\\ \rho&=\sqrt{\omega_r}\,r.\end{aligned} \tag{B.2}$$

Thus,

$$\left[-\frac{1}{2}\frac{d^2}{dr^2}+\frac{1}{2}\omega_r^2r^2+\frac{1}{2}\frac{1}{r}+\frac{(m^2-1/4)}{2}\frac{1}{r^2}\right]u(r)=\varepsilon'u(r). \tag{B.3}$$

The solution of the wave function has the form [14, 26, 27]

$$u(\rho)=e^{(-1/2)\rho^2}t(\rho), \tag{B.4}$$

where

$$t(\rho)=\rho^{|m|+1/2}\sum_{v=0}^{\infty}a_v\rho^v. \tag{B.5}$$

The coefficients in the series are related by the following recursion relation (note that there is also one normalization condition)

$$\begin{aligned} a_0 &\neq 0, \\ a_1 &= \frac{1}{2(|m|+1/2)\sqrt{\omega_r}} a_0, \\ a_v &= \frac{1}{v(v+2|m|)} \left\{ \frac{1}{\sqrt{\omega_r}} a_{v-1} + [2(v+|m|-1) - \varepsilon''] a_{v-2} \right\}. \end{aligned} \tag{B.6}$$

Define $a_v = a_0\, F(|m|, v, \varepsilon'', \omega_r)$ to be the recursion relation above. The termination of the series $t(\rho)$ at $n$ requires that

$$\begin{aligned} \varepsilon' &= (|m|+n)\omega_r, \\ F(|m|,&n, 2(|m|+n), \omega_r) = 0. \end{aligned} \tag{B.7}$$

and the wave function can be calculated straightforwardly.

## B.2 3D systems

Make the same change of variables as before and assume the ansatz

$$\varphi(\mathbf{r}) = \frac{u(r)}{r}\, Y_{lm}(\mathbf{r}). \tag{B.8}$$

The relative Hamiltonian reads

$$\left[ -\frac{1}{2}\frac{d^2}{dr^2} + \frac{1}{2}\omega_r^2 r^2 + \frac{1}{2}\frac{1}{r} + \frac{l(l+1)}{2}\frac{1}{r^2} \right] u(r) = \varepsilon' u(r). \tag{B.9}$$

The solution of the wave function has the form [14, 26, 27]

$$u(\rho) = e^{(-1/2)\rho^2} t(\rho), \tag{B.10}$$

where

$$t(\rho) = \rho^m \sum_{v=0}^{\infty} a_v \rho^v, \tag{B.11}$$

and $m = l + 1$. The coefficients in the series are related by the following recursion relation (note that there is also one normalization condition)

$$\begin{aligned} a_0 &\neq 0, \\ a_1 &= \frac{1}{2(l+1)\sqrt{\omega_r}} a_0, \\ a_v &= \frac{1}{v(v+2l+1)} \left\{ \frac{1}{\sqrt{\omega_r}} a_{v-1} + [2(l+v) - 1 - \varepsilon''] a_{v-2} \right\}. \end{aligned} \tag{B.12}$$

Define $F$ as before. we obtain

$$\begin{aligned} \varepsilon' &= \frac{[2(l+n)+1]\omega_r}{2}, \\ F(l,&n, 2(l+n)+1, \omega_r) = 0. \end{aligned} \tag{B.13}$$

and the wave function can be calculated straightforwardly.

Below are the complete energy spectra for the relative motion in 2D and 3D for the lowest 10 termination numbers $n$.

Table B.1: Quasi-exact solution pairs $(\omega_r, \epsilon')$ in 2D (left) and 3D (right) for termination number $n = 2$ to 10

| | $m=0$ | | $m=\pm1$ | |
|---|---|---|---|---|
| | $1/\omega_r$ | $\varepsilon'$ | $1/\omega_r$ | $\varepsilon'$ |
| $n=2$ | 2.000 | 1.000 | 6.000 | 0.500 |
| $n=3$ | 12.000 | 0.250 | 28.000 | 0.143 |
| $n=4$ | 37.088 | 0.108 | 72.558 | 0.069 |
| | 2.912 | 1.374 | 7.442 | 0.672 |
| $n=5$ | 84.467 | 0.059 | 146.604 | 0.041 |
| | 15.533 | 0.322 | 33.396 | 0.180 |
| $n=6$ | 161.253 | 0.037 | 257.194 | 0.027 |
| | 45.028 | 0.133 | 84.064 | 0.083 |
| | 3.719 | 1.614 | 8.742 | 0.801 |
| $n=7$ | 274.552 | 0.025 | 411.420 | 0.019 |
| | 98.700 | 0.071 | 166.224 | 0.048 |
| | 18.748 | 0.373 | 38.356 | 0.209 |
| $n=8$ | 431.472 | 0.019 | 616.386 | 0.015 |
| | 183.686 | 0.044 | 286.871 | 0.031 |
| | 52.381 | 0.153 | 94.799 | 0.095 |
| | 4.462 | 1.793 | 9.945 | 0.905 |
| $n=9$ | 639.123 | 0.014 | 879.199 | 0.011 |
| | 307.090 | 0.029 | 453.077 | 0.022 |
| | 112.038 | 0.080 | 184.721 | 0.054 |
| | 21.749 | 0.414 | 43.004 | 0.233 |
| $n=10$ | 904.617 | 0.011 | 1206.968 | 0.009 |
| | 476.020 | 0.021 | 671.937 | 0.016 |
| | 204.893 | 0.049 | 315.069 | 0.035 |
| | 59.309 | 0.169 | 104.949 | 0.105 |
| | 5.161 | 1.938 | 11.077 | 0.993 |

| | $l=0$ | | $l=1$ | |
|---|---|---|---|---|
| | $1/\omega_r$ | $\varepsilon'$ | $1/\omega_r$ | $\varepsilon'$ |
| $n=2$ | 4.000 | 0.625 | 8.000 | 0.438 |
| $n=3$ | 20.000 | 0.175 | 36.000 | 0.125 |
| $n=4$ | 54.739 | 0.082 | 90.448 | 0.061 |
| | 5.261 | 0.855 | 9.553 | 0.576 |
| $n=5$ | 115.299 | 0.048 | 178.147 | 0.036 |
| | 24.701 | 0.223 | 41.853 | 0.155 |
| $n=6$ | 208.803 | 0.031 | 306.069 | 0.025 |
| | 64.813 | 0.100 | 102.965 | 0.073 |
| | 6.384 | 1.018 | 10.966 | 0.684 |
| $n=7$ | 342.366 | 0.022 | 481.256 | 0.018 |
| | 132.638 | 0.057 | 199.476 | 0.043 |
| | 28.996 | 0.259 | 47.269 | 0.180 |
| $n=8$ | 523.102 | 0.016 | 710.785 | 0.013 |
| | 235.301 | 0.036 | 338.243 | 0.028 |
| | 74.177 | 0.115 | 114.689 | 0.083 |
| | 7.419 | 1.146 | 12.283 | 0.773 |
| $n=9$ | 758.124 | 0.013 | 1001.748 | 0.010 |
| | 379.925 | 0.025 | 526.252 | 0.020 |
| | 148.942 | 0.064 | 219.639 | 0.048 |
| | 33.009 | 0.288 | 52.361 | 0.201 |
| $n=10$ | 1054.542 | 0.010 | 1361.245 | 0.008 |
| | 573.625 | 0.018 | 770.552 | 0.015 |
| | 260.427 | 0.040 | 368.875 | 0.031 |
| | 83.015 | 0.126 | 125.801 | 0.091 |
| | 8.391 | 1.251 | 13.527 | 0.850 |

# C. Energy Spectrum of 1D Systems

The following tables show the energy spectrum of the systems corresponding to Fig.3.5, 3.6, and 3.7.

Table C.1: Total energy $E$ (in atomic units) for few-electron systems coupled to light with $\omega = 0.1$, $\lambda = 0.1$ (left), and $\omega_p = 1$ (right).

| | $\omega_p$ | $E$ (ECG) |
|---|---|---|
| $2e^-$ | | |
| S=1 | 0.1 | 0.534 |
| | 1 | 0.438 |
| | 2 | 0.418 |
| $3e^-$ | | |
| S=0.5 | 0.1 | 1.239 |
| | 1 | 1.172 |
| | 2 | 1.133 |
| S=1.5 | 0.1 | 1.222 |
| | 1 | 1.093 |
| | 2 | 1.055 |
| $4e^-$ | | |
| S=0 | 0.1 | 2.372 |
| | 1 | 2.348 |
| | 2 | 2.221 |
| S=2 | 0.1 | 2.186 |
| | 1 | 2.042 |
| | 2 | 1.974 |

| | $\lambda$ | $E$ (ECG) |
|---|---|---|
| $2e^-$ | | |
| S=1 | 0.1 | 0.438 |
| | 0.5 | 1.177 |
| | 1 | 2.732 |
| $3e^-$ | | |
| S=0.5 | 0.1 | 1.172 |
| | 0.5 | 3.205 |
| | 1 | 4.487 |
| S=1.5 | 0.1 | 1.093 |
| | 0.5 | 2.763 |
| | 1 | 4.374 |
| $4e^-$ | | |
| S=0 | 0.1 | 2.348 |
| | 0.5 | 4.981 |
| | 1 | 7.940 |
| S=2 | 0.1 | 2.042 |
| | 0.5 | 4.352 |
| | 1 | 7.615 |

# References


[1] Hannes Hübener et al. "Engineering quantum materials with chiral optical cavities". In: *Nature Materials* 20 (4 Apr. 2021), pp. 438–442. ISSN: 1476-1122. DOI: 10.1038/s41563-020-00801-7.

[2] Vasil Rokaj, Michael Ruggenthaler, Florian G. Eich, and Angel Rubio. "The Free Electron Gas in Cavity Quantum Electrodynamics". In: (June 2020).

[3] Christian Schäfer, Michael Ruggenthaler, and Angel Rubio. "¡i¿Ab initio¡/i¿ nonrelativistic quantum electrodynamics: Bridging quantum chemistry and quantum optics from weak to strong coupling". In: *Physical Review A* 98 (4 Oct. 2018), p. 043801. ISSN: 2469-9926. DOI: 10.1103/PhysRevA.98.043801.

[4] Dominik Sidler, Michael Ruggenthaler, Heiko Appel, and Angel Rubio. "Chemistry in Quantum Cavities: Exact Results, the Impact of Thermal Velocities, and Modified Dissociation". In: *The Journal of Physical Chemistry Letters* 11 (18 Sept. 2020), pp. 7525–7530. ISSN: 1948-7185. DOI: 10.1021/acs.jpclett.0c01556.

[5] Nicholas Rivera and Ido Kaminer. "Light–matter interactions with photonic quasiparticles". In: *Nature Reviews Physics* 2 (10 Oct. 2020), pp. 538–561. ISSN: 2522-5820. DOI: 10.1038/s42254-020-0224-2.

[6] Alexandre Le Boité. "Theoretical Methods for Ultrastrong Light–Matter Interactions". In: *Advanced Quantum Technologies* 3 (7 July 2020), p. 1900140. ISSN: 2511-9044. DOI: 10.1002/qute.201900140.

[7] Francisco J. Garcia-Vidal, Cristiano Ciuti, and Thomas W. Ebbesen. "Manipulating matter by strong coupling to vacuum fields". In: *Science* 373 (6551 July 2021). ISSN: 0036-8075. DOI: 10.1126/science.abd0336.

[8] M. Taut. "Two electrons in an external oscillator potential: Particular analytic solutions of a Coulomb correlation problem". In: *Physical Review A* 48 (5 Nov. 1993), pp. 3561–3566. ISSN: 1050-2947. DOI: 10.1103/PhysRevA.48.3561.

[9] M Taut. "Two electrons in a homogeneous magnetic field: particular analytical solutions". In: *Journal of Physics A: Mathematical and General* 27 (3 Feb. 1994), pp. 1045–1055. ISSN: 0305-4470. DOI: 10.1088/0305-4470/27/3/040.

[10] Pierre-François Loos and Peter M. W. Gill. "Two Electrons on a Hypersphere: A Quasiexactly Solvable Model". In: *Physical Review Letters* 103 (12 Sept. 2009), p. 123008. ISSN: 0031-9007. DOI: 10.1103/PhysRevLett.103.123008.

[11] Pierre-François Loos and Peter M.W. Gill. "Excited states of spherium". In: *Molecular Physics* 108 (19-20 Oct. 2010), pp. 2527–2532. ISSN: 0026-8976. DOI: 10.1080/00268976.2010.508472.

[12] Pierre-François Loos and Peter M. W. Gill. "Exact Wave Functions of Two-Electron Quantum Rings". In: *Physical Review Letters* 108 (8 Feb. 2012), p. 083002. ISSN: 0031-9007. DOI: 10.1103/PhysRevLett.108.083002.

[13] GUANG-JIE GUO, ZHONG-ZHOU REN, BO ZHOU, and XIAO-YONG GUO. "QUASI-EXACTLY ANALYTICAL SOLUTIONS OF TWO ELECTRONS IN VERTICALLY COUPLED RINGS". In: *International Journal of Modern Physics B* 26 (32 Dec. 2012), p. 1250201. ISSN: 0217-9792. DOI: 10.1142/S0217979212502013.

[14] M Taut. "Two-dimensional hydrogen in a magnetic field: analytical solutions". In: *Journal of Physics A: Mathematical and General* 28 (7 Apr. 1995), pp. 2081–2085. ISSN: 0305-4470. DOI: 10.1088/0305-4470/28/7/026.

[15] Michael Ruggenthaler et al. "From a quantum-electrodynamical light–matter description to novel spectroscopies". In: *Nature Reviews Chemistry* 2 (3 Mar. 2018), p. 0118. ISSN: 2397-3358. DOI: 10.1038/s41570-018-0118.

[16] Vasil Rokaj, Davis M Welakuh, Michael Ruggenthaler, and Angel Rubio. "Light–matter interaction in the long-wavelength limit: no ground-state without dipole self-energy". In: *Journal of Physics B: Atomic, Molecular and Optical Physics* 51 (3 Feb. 2018), p. 034005. ISSN: 0953-4075. DOI: 10.1088/1361-6455/aa9c99.

[17] I. V. Tokatly. "Conserving approximations in cavity quantum electrodynamics: Implications for density functional theory of electron-photon systems". In: *Physical Review B* 98 (23 Dec. 2018), p. 235123. ISSN: 2469-9950. DOI: 10.1103/PhysRevB.98.235123.

[18] Arkajit Mandal, Sebastian Montillo Vega, and Pengfei Huo. "Polarized Fock States and the Dynamical Casimir Effect in Molecular Cavity Quantum Electrodynamics". In: *The Journal of Physical Chemistry Letters* 11 (21 Nov. 2020), pp. 9215–9223. ISSN: 1948-7185. DOI: 10.1021/acs.jpclett.0c02399.

[19] Arkajit Mandal, Todd D. Krauss, and Pengfei Huo. "Polariton-Mediated Electron Transfer via Cavity Quantum Electrodynamics". In: *The Journal of Physical Chemistry B* 124 (29 July 2020), pp. 6321–6340. ISSN: 1520-6106. DOI: 10.1021/acs.jpcb.0c03227.

[20] Edwin Power and S Zienau. "Coulomb gauge in non-relativistic quantum electro-dynamics and the shape of spectral lines". In: *Philosophical Transactions of the Royal Society of London. Series A, Mathematical and Physical Sciences* 251 (999 Sept. 1959), pp. 427–454. ISSN: 0080-4614. DOI: 10.1098/rsta.1959.0008.

[21] Kalman Varga and Joseph A. Driscoll. *Computational Nanoscience*. Cambridge University Press, 2011. ISBN: 9780511736230. DOI: 10.1017/CBO9780511736230.

[22] Vasil Rokaj, Davis M Welakuh, Michael Ruggenthaler, and Angel Rubio. "Light–matter interaction in the long-wavelength limit: no ground-state without dipole self-energy". In: *Journal of Physics B: Atomic, Molecular and Optical Physics* 51 (3 Feb. 2018), p. 034005. ISSN: 0953-4075. DOI: 10.1088/1361-6455/aa9c99.

[23] Chenhang Huang, Alexander Ahrens, Matthew Beutel, and Kálmán Varga. "Two electrons in harmonic confinement coupled to light in a cavity". In: *Physical Review B* 104 (16 Oct. 2021), p. 165147. ISSN: 2469-9950. DOI: 10.1103/PhysRevB.104.165147.

[24] José Zúñiga, Adolfo Bastida, and Alberto Requena. "Quantum solution of coupled harmonic oscillator systems beyond normal coordinates". In: *Journal of Mathematical Chemistry* 55 (10 Nov. 2017), pp. 1964–1984. ISSN: 0259-9791. DOI: 10.1007/s10910-017-0777-1.

[25] Chenhang Huang, Daniel Pitagora, Timothy Zaklama, and Kálmán Varga. "Energy spectrum and structure of confined one-dimensional few-electron systems with and without coupling to light in a cavity". In: *Physical Review A* 104 (4 Oct. 2021), p. 043109. ISSN: 2469-9926. DOI: 10.1103/PhysRevA.104.043109.

[26] M. Taut. "Two electrons in an external oscillator potential: Particular analytic solutions of a Coulomb correlation problem". In: *Physical Review A* 48 (5 Nov. 1993), pp. 3561–3566. ISSN: 1050-2947. DOI: 10.1103/PhysRevA.48.3561.

[27] M Taut. "Two electrons in a homogeneous magnetic field: particular analytical solutions". In: *Journal of Physics A: Mathematical and General* 27 (3 Feb. 1994), pp. 1045–1055. ISSN: 0305-4470. DOI: 10.1088/0305-4470/27/3/040.